

2005
Annual Conference
Structural Stability Research Council
Montreal, Canada

**UNDERSTANDING AND CLASSIFYING
LOCAL, DISTORTIONAL AND GLOBAL
BUCKLING IN OPEN THIN-WALLED
MEMBERS**

B.W. Schafer¹ and S. Ádány²

ABSTRACT

Cross-section instability greatly complicates the behavior of thin-walled members. Current computational stability techniques do little to add clarity. The terms “global,” “distortional,” and “local buckling” permeate the literature, but there are no satisfactory definitions for the three characteristic modes. Despite this, design standards require the calculation of buckling stresses, as each characteristic mode has a differing degree of post-buckling capacity, and may trigger a different collapse response. Further, interaction between all modes is possible, but poorly understood. This paper proposes a new approach for buckling mode definitions of open cross-section thin-walled members, which, unlike the existing heuristic definitions, are based on simple mechanical assumptions which can easily be applied in the context of any numerical method. The application of the proposed definitions to the Finite Strip Method is briefly demonstrated. The technique may be used either to classify results after performing an analysis (including the extent of interaction) or to constrain a model to a particular characteristic mode or modes before performing the analysis. Numerical examples are provided to justify the applicability and efficiency of the proposed classification

¹ Department of Civil Engineering, Johns Hopkins University,
Baltimore, MD, USA <schafer@jhu.edu>

² Department of Structural Mechanics, Budapest University of Tech.
and Economics, Budapest, Hungary <sadany@epito.bme.hu>

INTRODUCTION

Thin-walled members, if subjected to compressive normal stresses over all or part of the cross-section most frequently fail by loss of stability. Usually three basic modes, or classes, of buckling phenomena can be distinguished: (i) local, (ii) distortional, and (iii) global buckling. Any of these modes may lead to excessive deformation and, finally, to failure. Each mode has a differing degree of post-buckling capacity and often trigger different collapse response, thus, it is important to properly calculate the critical stress associated with the various modes to avoid the loss of stability. The importance of buckling on the ultimate behaviour is also reflected in current design codes which, directly or indirectly, use the member critical stress, or load, to determine the resistance. (e.g., see [1,2,3,4])

Although the design standards require the calculation of buckling stresses, and although the terms global, distortional and local buckling are extensively used in the literature, there is no generally applicable method which provides buckling stresses for all the three characteristic modes. Further, there are no widely adopted and clear definitions for the various modes themselves.

The first part of this paper will highlight existing problems as they relate to buckling mode definition and calculation. Then, definitions will be proposed for the three basic modes, which were applied by the authors, in the context of Finite Strip Method, for two basic problems: (i) pure mode calculation and (ii) mode classification. Finally, examples will be presented to illustrate the capabilities of the proposed definitions.

Problems of mode definition and calculation

Mode definition

General and widely adopted definitions for thin-walled buckling modes do not currently exist; however, the following definitions may be considered as the most commonly used:

- global buckling is a buckling mode where the member deforms with no deformation in its cross-sectional shape, consistent with classical beam theory;
- local buckling is normally defined as the mode which involves plate-like deformations alone, without the translation of the intersection lines of adjacent plate elements;
- distortional buckling is a mode with cross-sectional distortion that involves the translation of some of the fold lines (intersection lines of adjacent plate elements).

Other considerations in typical use relate to the wavelength of the buckling mode, and to discussion of membrane vs. flexural plate deformations. The preceding definitions work well for a number of practical problems; however, they are not exact enough in many other cases. Two typical examples are mentioned here.

Figure 1a presents a cold-formed steel channel section with a small lip stiffener. Both the presented buckled shape and the associated critical load are nearly identical with those of a similar unlipped channel. However, while the buckled shape of an unlipped channel is most frequently classified as local, if we employ the previous definitions the same buckling mode of a cross-section with a small stiffener should be classified as distortional. Note, even in the case of an unlipped channel there are reasons (length of the buckling mode, failure mechanism) to classify the presented mode as distortional instead of local.

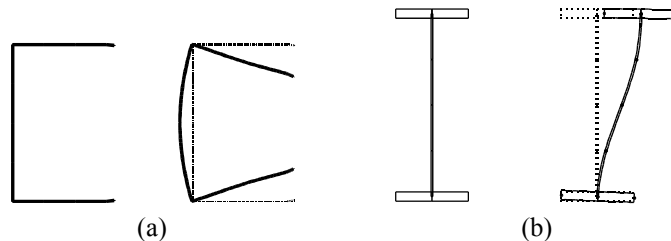


Figure 1: Examples for uncertainty in buckling mode definitions

Figure 1b shows a symmetrical I-section, together with a possible buckled shape which can occur if the member is loaded as a beam. It is clear that the presented buckled shape can neither be pure local nor

pure global, since the cross-section is distorted and at least one of the intersection lines is displaced. From this aspect one might classify the buckling mode as distortional, and indeed this has been done in many cases. Other theoretical considerations (e.g., Generalised Beam Theory, discussed later in this paper), however imply that I-sections do not have distortional buckling modes. Further examples can be found in [5].

Buckling load calculation

Analytical formulae for the calculation of the buckling load in all modes (global, distortional, and local) either do not exist, are too cumbersome, or are too limited in their applicability to provide a general tool. Here, three numerical methods are considered for buckling load calculation: the Finite Element Method, the Finite Strip Method, and Generalised Beam Theory. While these approaches can be regarded as the most efficient and widely used ways to determine critical loads, each numerical method has certain limitations.

The Finite Element Method (FEM) is by far the most popular and general numerical method. FEM is applicable to practically any kind of structural member, any loading, and any boundary condition. In addition, there are a large number of available software packages. The price of this general applicability is the relatively large number of required finite elements, which is not only computationally demanding, but results in a large number of possible buckling modes, among which FEM cannot automatically distinguish. Thus, it is the user who must classify the calculated modes, typically largely on the basis of a visual analysis of the deformed buckling mode shapes, which is a time-consuming and highly subjective process.

The available Finite Strip Method (FSM) software packages ([6,7]) try to overcome FEM's identification problem by automatic determination of the critical stress/load as a function of buckling length. This helps the user to identify the characteristic buckling modes, since, in many cases, the first minimum point of the curve identifies the local buckling, while the second minimum point is often associated with the distortional buckling mode. An example is presented in Figure 2 (upper

curve) for a simple lipped channel column, where the buckling load (P_{cr}) is non-dimensionalized by dividing by the squash load (P_y). Examples exist where FSM does not automatically identify minima, and this identification method fails. Figure 2 also shows a curve (lower), again for a simple lipped channel column, where only one (local) minimum point exists, while the distortional minimum does not exist. Finally, as typically implemented, FSM is limited in its applicability to prismatic members and simple boundary conditions.

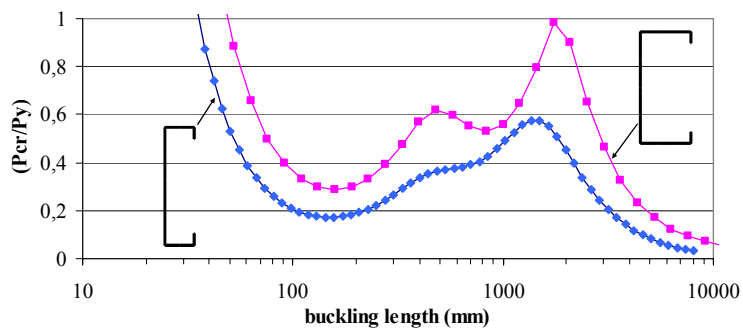


Figure 2: Critical loads of C-section columns

Recently, Generalised Beam Theory (GBT) has been applied to the buckling analysis of prismatic thin-walled members ([8,9,10,11,12]). The attractive feature of GBT is its capability to categorize the buckling modes automatically, and directly provide the buckling stresses that are required for design. However, GBT introduces special simplifying assumptions for the deformations which limits its applicability, the formulation is somewhat unconventional and not readily apparent to users of more common FEM approaches, and software packages for GBT are not widely available for potential users.

Thus, it would be useful to develop a generally applicable procedure for buckling load calculation and identification, without the uncertainties, and disadvantages of existing methods. This, however, requires more exact definitions for the buckling modes.

Mode definitions based on The Generalised Beam Theory

General

GBT is the only known method which is able to produce and isolate solutions for all the buckling modes: global, distortional and local. Further, modes identified via the GBT methodology are generally in accordance with the definitions mentioned in Section 2.1. Thus, our aim is to identify the critical assumptions in the GBT formulation that lead to the method's ability to isolate the modes. However, the goal is not to mimic the GBT formulation, but rather to construct the underlying GBT ideas as a series of distinct mechanical assumptions. These mechanical assumptions can then be enforced through constraints in more general methods such as FSM or FEM. Application to FSM will be illustrated here.

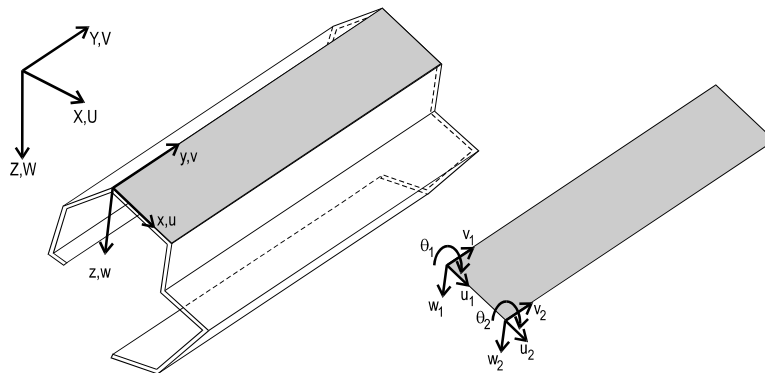


Figure 3: Coordinate systems and DOFs

Mode definitions

Based on an analysis of the GBT methodology, we put forth the following criteria as the critical mechanical assumptions necessary for defining the buckling modes. (Coordinate system as in Figure 3.)

Criterion #1, membrane deformations:

- $\gamma_{xy} = 0$, membrane (in-plane) shear strains are zero,
- $\epsilon_x = 0$, membrane transverse strains are zero, and
- $v = f(x)$, long. displacements are linear in x within an element.

Criterion #2, longitudinal warping,

- $\varepsilon_y \neq 0$, long. strains/displacements are non-zero along the length.

Criterion #3, transverse flexure,

- $\kappa_y = 0$, no flexure in the transverse direction.

The buckling modes can then be defined as follows (see also Table 1).

- *Global* modes are those deformation patterns that satisfy all three criteria.
- *Distortional* modes are those deformation patterns that satisfy criteria #1 and #2, but do not satisfy criterion #3 (i.e., transverse flexure occurs).
- *Local* modes are those deformation patterns that satisfy criterion #1, but do not satisfy criterion #2 (i.e., no longitudinal warping occurs) while criterion #3 is irrelevant.
- If a deformation pattern does not satisfy criterion #1, it should be classified as *other* mode (independently of the other criteria). Note, other modes do not exist in GBT, but must exist in FSM or FEM due to the inclusion of degrees of freedom (DOFs) for the membrane.

Table 1: Mode classification table

	G modes	D modes	L modes	O modes
$\gamma_{xy} = 0, \varepsilon_x = 0, v$ is linear	Yes	Yes	Yes	No
$\varepsilon_y \neq 0$	Yes	Yes	No	-
$\kappa_y = 0$	Yes	No	-	-

Introduction of the definitions into the Finite Strip Method

General

The application of the above definitions implies that the appropriate deformation constraints, which are formulated in the three criteria, must be introduced into FSM. As a consequence, the original number of degrees of freedom (DOF) is necessarily reduced since the member can only deform in accordance with the strain conditions. Thus, our goal is

to work out how the DOFs are reduced due to the various strain assumptions, and how this DOF reduction can practically be handled. Although the derivations are not extremely complicated, they are much longer than the limits provided by this paper. For this reason, here only a small example will be presented to demonstrate the method, which, at the same time, highlights all the important features of the more general derivations. Complete derivations can be found in [5].

Constraint matrix derivation

Consider the membrane deformation of a single finite strip, as shown in Figure 3. If the longitudinal distributions are assumed to be sinusoidal, as in the classical implementations of FSM, e.g., see [6] for CUFSM, the displacements can be expressed as a product of the assumed shape functions and the nodal displacements.

$$u(x, y) = \begin{bmatrix} \left(1 - \frac{x}{b}\right) & \left(\frac{x}{b}\right) \end{bmatrix} \begin{bmatrix} u_1 \\ u_2 \end{bmatrix} \sin \frac{m\pi y}{a} \quad (1)$$

$$v(x, y) = \begin{bmatrix} \left(1 - \frac{x}{b}\right) & \left(\frac{x}{b}\right) \end{bmatrix} \begin{bmatrix} v_1 \\ v_2 \end{bmatrix} \cos \frac{m\pi y}{a} \quad (2)$$

where u_1 , u_2 , v_1 , v_2 are the transverse and longitudinal nodal displacements, m is the number of half-sine waves in the longitudinal direction, and a and b are the length and width of the strip, respectively. Note, there are 4 nodal displacements, i.e. the number of DOFs = 4.

Let us now introduce the criteria for zero transverse membrane strains:

$$\varepsilon_x = \frac{\partial u}{\partial x} = 0 \quad (3)$$

Substituting Eq. (1) into Eq. (3):

$$\varepsilon_x = \frac{\partial u}{\partial x} = \frac{-u_1 + u_2}{b} \sin \frac{m\pi y}{a} = 0 \quad (4)$$

and since the sine function is generally not equal to zero, u_1 and u_2 must be equal to each other in order to satisfy the equality.

This implies that the transverse displacements of the strip's two nodal lines must be identical, which is a natural consequence of the zero transverse strain assumption. In practice, the identical u displacements prevent those deformations where the two longitudinal edges of the strip are not parallel, as illustrated in Figure 4.

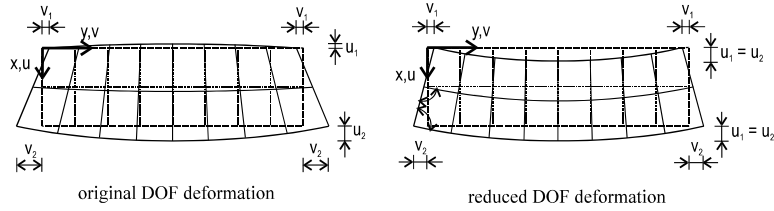


Figure 4: Effect of $\epsilon_x = 0$ strain constraint on membrane deformations

The above derivation demonstrates that the introduction of a strain constraint reduces the number of DOFs, in this particular case from 4 to 3. Thus, we can define the new, reduced DOFs by u , v_1 and v_2 , while the relationship of the original and reduced displacement vectors can be expressed as follows:

$$\begin{bmatrix} u_1 \\ v_1 \\ u_2 \\ v_2 \end{bmatrix} = \begin{bmatrix} 1 & 0 & 0 \\ 0 & 1 & 0 \\ 1 & 0 & 0 \\ 0 & 0 & 1 \end{bmatrix} \begin{bmatrix} u \\ v_1 \\ v_2 \end{bmatrix} \quad (5)$$

or in short:

$$\mathbf{d} = \mathbf{R}\mathbf{d}_r \quad (6)$$

where \mathbf{R} is the constraint matrix, which is a representation of the introduced strain constraints.

In case of the more general strain-displacement constraints, and more general cross-sections, the derivations are somewhat more complicated, but finally the associated constraint matrices (\mathbf{R}) can be defined, as shown in [5] and apply for all the criterion summarized in Table 1.

Application of constraint matrices

As Eq. (6) shows, the constraint matrices define the relationship between the original DOFs and the reduced DOFs. Let us consider the static equilibrium of a single strip:

$$\mathbf{Kd} = \mathbf{f} \quad (7)$$

where \mathbf{K} is the stiffness matrix, \mathbf{d} is the displacement vector, and \mathbf{f} is the vector of nodal forces. By substituting Eq. (6) into Eq. (7), and pre-multiplying by \mathbf{R}^T :

$$\mathbf{R}^T \mathbf{K} \mathbf{R} \mathbf{d}_r = \mathbf{R}^T \mathbf{f} \quad (8)$$

For our example, let us calculate the right-hand side Eq. (8):

$$\mathbf{R}^T \mathbf{f} = \begin{bmatrix} 1 & 0 & 1 & 0 \\ 0 & 1 & 0 & 0 \\ 0 & 0 & 0 & 1 \end{bmatrix} \begin{bmatrix} F_{u1} \\ F_{v1} \\ F_{u2} \\ F_{v2} \end{bmatrix} = \begin{bmatrix} F_{u1} + F_{u2} \\ F_{v1} \\ F_{v2} \end{bmatrix} = \mathbf{f}_r \quad (9)$$

Thus, $\mathbf{R}^T \mathbf{f}$ can be interpreted as the nodal forces corresponding to the new reduced DOFs. The $\mathbf{R}^T \mathbf{K} \mathbf{R}$ term on the left-hand side of Eq. (8) is the stiffness matrix associated with the reduced DOF problem, $\mathbf{K}_r = \mathbf{R}^T \mathbf{K} \mathbf{R}$.

The same constraint matrix (\mathbf{R}) can be applied for displacement vectors and force vectors to perform transformation between the reduced DOF problem and the original DOF problem. Moreover, the same constraint matrix may be used to define the stiffness matrix of the reduced DOF problem once the un-constrained stiffness matrix is determined.

Application

Pure mode calculation

By the application of constraints associated with the strain assumptions of the various modes as described in Table 1, the problem of pure buckling mode calculation can be solved. Instead of solving the generalized eigenvalue problem of the member:

$$\mathbf{K}\mathbf{d} = \lambda\mathbf{K}_g\mathbf{d} \quad (10)$$

where \mathbf{K}_g is the geometric stiffness matrix and λ is the eigenvalue, one solves the reduced (or constrained) problem::

$$\mathbf{K}_r\mathbf{d} = \lambda\mathbf{K}_{gr}\mathbf{d} \quad (11)$$

where $\mathbf{K}_r = \mathbf{R}^T\mathbf{K}\mathbf{R}$ and $\mathbf{K}_{gr} = \mathbf{R}^T\mathbf{K}_g\mathbf{R}$ are the elastic and geometric stiffness matrix of the reduced DOF problem, respectively. The eigenvectors (buckling modes) correspond to the given deformation modes defined in Table 1.

Mode contribution calculation

It is desired to understand how the different pure modes of Eq. (11) for global, distortional, local, and other mode buckling contribute in an all-mode or traditional FSM calculation, i.e. Eq. (10). This is completed by transforming any displaced shape (buckled mode shape) into the eigenbasis created by the pure mode solution of Eq. (11). The eigenvectors \mathbf{d} from the solution to Eq. (11) fully describe the pure mode solutions. Eq. (6) provides transformation from (or to) the pure mode space to the original DOF space.

The basis vectors must be normalized. Here, we select a normalization so that each base vector is associated with unit strain energy. In practice, let us consider again the eigenvalue problem of the member, as defined by Eq. (10). Any orthogonalized base vector satisfies Eq. (10), thus, we may write:

$$\mathbf{K}\mathbf{d}_0 = \lambda\mathbf{K}_g\mathbf{d}_0 \quad (12)$$

where \mathbf{d}_o denotes the orthogonalized base vector. By pre-multiplying Eq. (12) with $\frac{1}{2}\mathbf{d}_o^T$:

$$\frac{1}{2}\mathbf{d}_o^T \mathbf{K} \mathbf{d}_o = \frac{1}{2}\lambda \mathbf{d}_o^T \mathbf{K}_g \mathbf{d}_o \quad (13)$$

where the left-hand side of the equation is the elastic strain energy, which by scaling the \mathbf{d}_o vector can be set to unity.

Any displacement vector can now be expressed as a linear combination of the basis vectors, by solving the linear matrix-equation as follows:

$$\mathbf{D}_o \mathbf{c} = \mathbf{d} \quad (14)$$

where \mathbf{D}_o is a square matrix constructed from the orthonormal \mathbf{d}_o base vectors so that each column of \mathbf{D}_o would be a base vector; \mathbf{d} is the given general displacement vector, while \mathbf{c} is a vector containing the coefficients which are to be calculated. The contribution of any individual mode can be calculated as the ratio of the coefficient of that mode and the sum of all the coefficients, as follows:

$$|c_i| / \sum_{\text{all}} |c_i| \quad (15)$$

Similarly, the contribution of a mode class can be defined as:

$$\sum_{\text{mode}} |c_i| / \sum_{\text{all}} |c_i| \quad (16)$$

Numerical examples

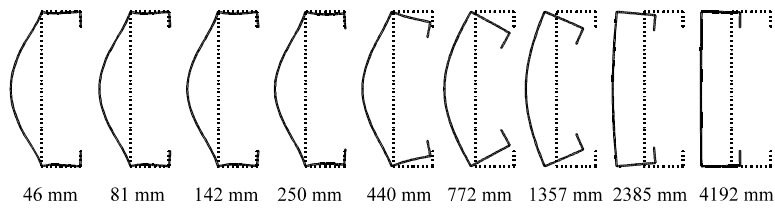
Several illustrative examples are presented here, calculated by the CUFISM software applying the mode definitions and base functions described in this paper, and detailed in [5].

Lipped channel in compression (Figure 5): the example demonstrates a case where the all-mode FSM calculation has an indistinct distortional minimum. Pure mode calculations provide solutions for the individual

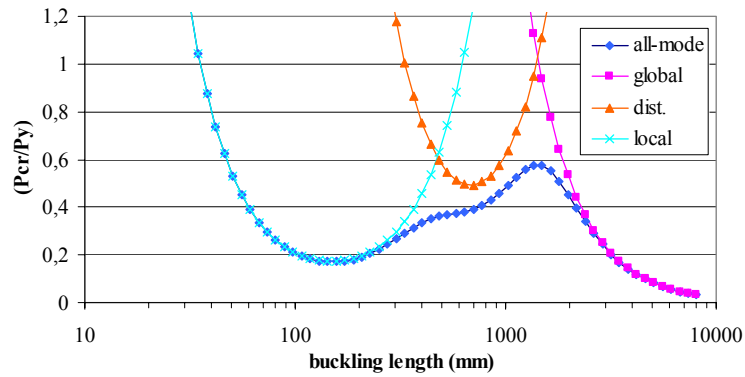
modes, and demonstrate that interaction is causing a reduction in the buckling load below the pure distortional mode prediction. The modal contributions of Figure 5c quantify the level of local and global buckling interaction with the distortional mode. The contribution of “other” modes is practically zero, implying that criterion #1 ($\gamma_{xy} = 0$, $\epsilon_x = 0$, v is linear) is automatically satisfied for this particular problem. According to the experiences of the authors this is true for many practical problems which justifies the applicability of GBT for many practical cases. Note, however, it is easy to find examples where the contribution of other modes is not negligible.

Lipped Channel with a web stiffener in compression (Figure 6): the example demonstrates the case where two distortional minima occur. As Figure 6a shows, distortional buckling of the web (Figure 6a – 250mm), and distortional buckling of the web+flange (Figure 6a – 772mm) occur as two separate minima in the all-mode FSM analysis, and in the pure mode distortional analysis. The “distortional” buckling of the web is behaviourally similar to local buckling of a lipped channel without a web stiffener (e.g., Figure 5a – 142mm), but due to the presence of the web stiffener is identified as distortional, as shown in Figure 6c. In fact, as detailed in [5], no matter how small the web stiffener size is, the developed method will identify modes involving translation of the web stiffener as distortional. This leads to a conflict between definitions of local and distortional buckling. A similar situation occurs in our final example regarding lip stiffeners.

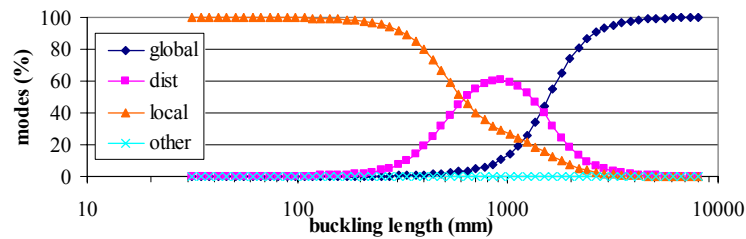
I-section in bending (Figure 7): the example demonstrates distortional buckling of I-sections, as shown in Figure 7a – 794mm, may be classified as local-global coupling. To fully understand this analysis the complete derivations in [5] are helpful; however, a key characteristic of distortional buckling is that it may be completely defined by the axial warping displacements of the cross-section. An I-section has only two independent main nodal lines (the web/flange junctures) and these are completely defined by the lateral and torsional warping displacements. It is also perhaps interesting to note in Figure 7c that local coupling with global buckling is fairly significant unless the beam is quite long.



(a) all-mode, buckled shapes for increasing half-wavelength

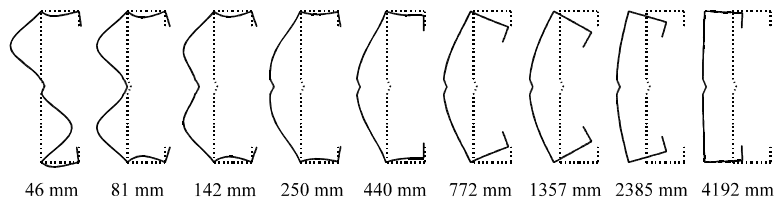


(b) all-mode and pure mode calculations

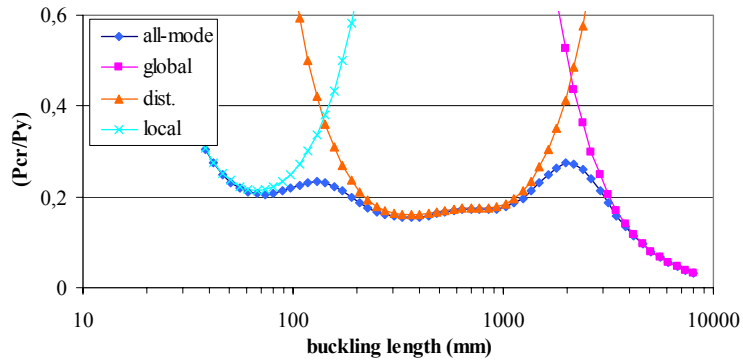


(c) mode contributions to all-mode buckling

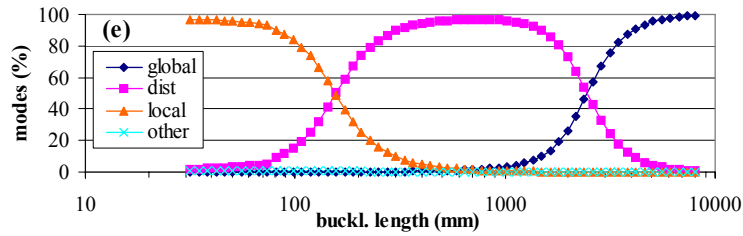
Figure 5: Buckling analysis of a lipped channel section
(200mm x 50mm x 20mm x 1.5 mm)



(a) all-mode, buckled shapes for increasing half-wavelength

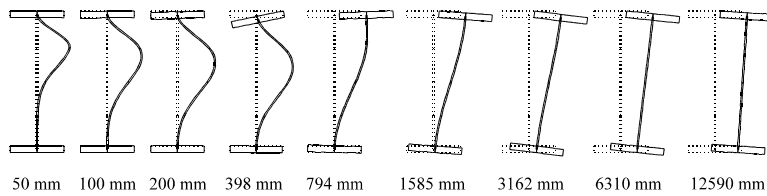


(b) all-mode and pure mode calculations

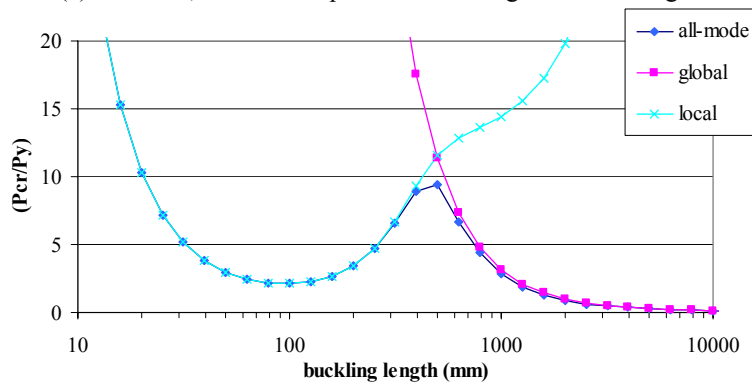


(c) mode contributions to all-mode buckling

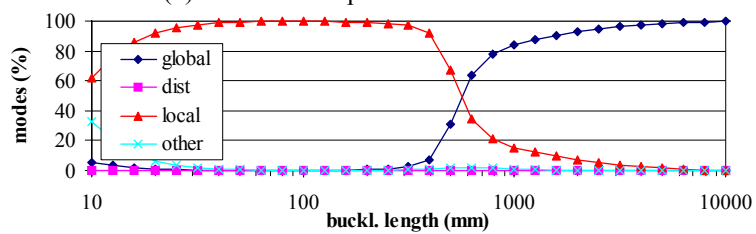
Figure 6: Buckling analysis of a lipped channel with web stiffener (200mm x 50mm x 20mm x 0.75 mm, stiffener 20mm x 4.5mm)



(a) all-mode, buckled shapes for increasing half-wavelength

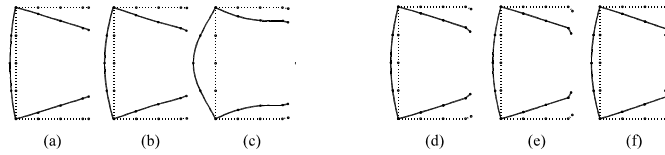


(b) all-mode and pure mode calculations

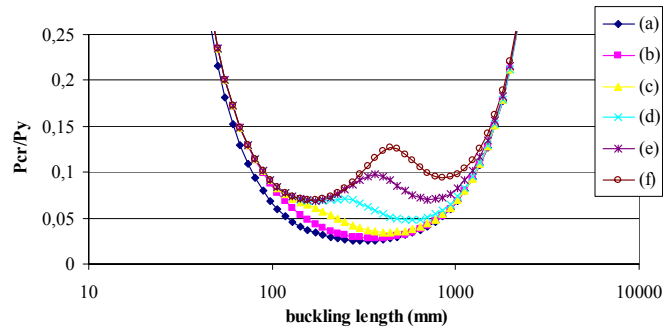


(c) mode contributions to all-mode buckling

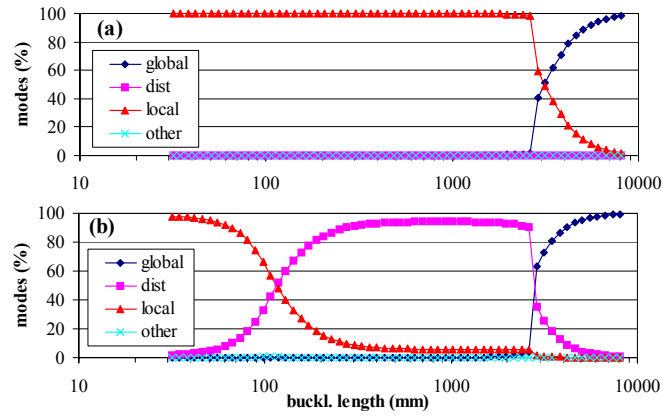
Figure 7: Buckling analysis of an I section (200mm deep, 80mm flanges, $t_w=2\text{mm}$, $t_f=10\text{mm}$)



(a) selected buckled shapes for varying lip stiffener angle
 (half-wavelength: a-c at 170mm, d-f at distortional min ~ 700mm)



(b) combined local and distortional mode calculations for varied lip θ



(c) mode contributions to all-mode buckling for members a and b only

Figure 8: Analysis of a lipped channel with varying stiffener angle
 (200mm x 120mm x 10mm x 1mm, 10mm lip varies from 0° to 90°)

Lipped channel with varying stiffener angle (Figure 8): the example demonstrates the difficulty with defining the difference between local and distortional buckling; even with the criteria developed herein. Unlike in the previous examples, this example is for a series of different cross-sections. A small lip stiffener is systematically varied from an angle of 0° to 90° (sections a – f in Figure 8). The results show that as the lip approaches 90° the FSM solution provides distinct local and distortional minima, but for small lip angles the two modes are indistinct. Comparing the modal identification for lip angles at 0° and 18° (sections a and b) in Figure 8c shows that for 0° the section is identified as undergoing local buckling, while for a lip of 18° and visually the same buckling mode present, distortional buckling is identified. The two FSM curves (for sections a and b) are also nearly coincident. This behaviour is a direct result of the method used here, in defining the nodes that may contribute to warping of the cross-section, a key criterion is that the relative angle between two elements is non—zero. Section b meets this criterion and thus the mode shape of Figure 8a – Section b is developed entirely based on the warping DOF, while that of Figure 8a – Section a is not.

CONCLUDING REMARKS

A new approach is proposed in the paper for the buckling analysis of thin-walled members. Clear definitions for the buckling modes are proposed on the basis of simple mechanical assumptions. The applicability of the definitions to numerical methods is demonstrated in the context of the Finite Strip Method. The main advantage of the proposed method is that it makes possible the direct calculation of pure buckling modes, as well as the determination of mode contributions in coupled modes within numerical methods like FSM or FEM. The results can directly be used for standardised calculations, and may be the starting point to the development of more efficient design procedures.

ACKNOWLEDGEMENTS

The presented research has been performed under the partial support of the Imre Korányi Scholarship of the Thomas Cholnoky Foundation and the OTKA T035147 project of the Hungarian Scientific Research Fund.

REFERENCES

- [1] Eurocode 3, EN 1993-1-3, General rules, Supplementary rules for cold-formed thin gauge members and sheeting , Draft Version, September 27, 2002.
- [2] NAS, North American Specification for the Design of Cold-Formed Steel Structural Members. American Iron and Steel Institute, Canadian Standards Association, CANACERO, 2001.
- [3] Design of Cold-Formed Steel Structural Members using the Direct Strength Method, Appendix 1 of the NAS, 2004. (available also at http://www.ce.jhu.edu/bschafer/direct_strength)
- [4] AS/NZS 4600, Australian/New Zealand Standard, Cold-Formed Steel Structures, 1998.
- [5] Ádány, S: Buckling mode classification of members with open thin-walled cross-sections by using the Finite Strip Method, Research Report, Johns Hopkins University, 2004. (available at <http://www.ce.jhu.edu/bschafer>)
- [6] CUFSM v2.6, Elastic Buckling Analysis of Thin-Walled Members by Finite Strip Analysis, <http://www.ce.jhu.edu/bschafer/cufsm>
- [7] Thin-Wall v2.1, Cross-Section Analysis and Finite Strip Analysis and Direct Strength Design of Thin-Walled Structures, Centre for Advanced Structural Engineering, University of Sydney, <http://www.civil.usyd.edu.au/case/thinwall>
- [8] Schardt, R.: Verallgemeinerte Technische Biegetheorie, Springer Verlag, Berlin, 1989. (in German)
- [9] Davies, J.M., Leach, P.: First-order generalised beam theory, J. of Construct. Steel Res., 31(2-3), 1994, pp. 187-220.
- [10] Davies, J.M., Leach, P., Heinz, D.: Second-order generalised beam theory, J. of Construct. Steel Res., 31(2-3), 1994, pp. 221-241.
- [11] Silvestre, N., Camotim, D.: First-order generalised beam theory for arbitrary orthotropic materials, Thin-Walled Structures, 40, 2002, 755-789.
- [12] Silvestre, N., Camotim, D.: Second-order generalised beam theory for arbitrary orthotropic materials, Thin-Walled Structures, 40, 2002, 791-820.

KEYWORD INDEX

local buckling	1-7, 11, 13, 18
distortional buckling	1-7, 11-13, 17-18
global buckling	1-4, 6-7, 11, 13
generalised beam theory (GBT)	4-7, 13
finite strip method (FSM)	1-2, 4-8, 11, 13, 18

REFERENCE INDEX

[1] Eurocode (2002)	2
[2] NAS (2001)	2
[3] NAS (2004)	2
[4] AS/NZS (1998)	2
[5] Ádány (2004)	4, 8, 12, 13
[6] CUFSM (2004)	4, 8
[7] Thin-Wall (2004)	4
[8] Schardt (1989)	5
[9] Davies and Leach (1994)	5
[10] Davies, and Leach (1994b)	5
[11] Silvestre and Camotim (2002)	5
[12] Silvestre and Camotim (2002)	5